

# Fracture Mechanics Analysis and Strength Prediction of Carbon Fiber Composite Laminate with a Delamination

Chirag D Soni<sup>1</sup>, P K Sahoo<sup>2</sup>, S Srinivasan<sup>3</sup>, Santosh K<sup>4</sup>

<sup>#</sup>*Department of Aeronautical Engineering, MVJ College of Engineering, Visveswaraya Technological University Channasandra, Near ITPB, Bangalore-67, Karnataka, India*

<sup>1</sup>[chiragdsoni@gmail.com](mailto:chiragdsoni@gmail.com)

<sup>3</sup>[ssv.aero@gmail.com](mailto:ssv.aero@gmail.com)

<sup>2&4</sup>*National Aerospace Laboratories  
Kodihalli, Bangalore-17, Karnataka, India*

<sup>2</sup>[pks@nal.res.in](mailto:pks@nal.res.in)

<sup>4</sup>[santhu.hpt@gmail.com](mailto:santhu.hpt@gmail.com)

**Abstract**— The use of advanced carbon fibre-reinforced composites in aircraft primary structures has been steadily increasing over past two decades due to their high specific strength and stiffness, and their tailoring as per the need. The composite panels used in primary structures of aircraft are liable to be buckling during its service periods. It is observed that structures can withstand substantial amount of loads after they have buckled. Therefore, an approach to efficiently design the postbuckled composite structures is required to be developed. The designers of the next generation of aircraft are looking into the aspect of postbuckling composite structures to achieve substantial improvements in aircraft structural efficiency. In this work, the postbuckling response and growth of circular delamination in flat and curved composite plates are investigated for different delamination sizes and their locations through the laminate thickness. The prediction of delamination initiation and growth is carried out using the strain energy release rates obtained from the finite element analysis and comparing them to B-K's mixed-mode fracture criterion. The failure load is thus predicted. Predicted results for onset of delamination growth compared well with experimental results. Its variation with different delamination sizes and their locations across panel thickness was also investigated. It is observed that the failure loads are influenced by the delamination sizes depending on their locations across the laminate thickness. The different delamination sizes at H/3 laminate thickness did not have significant effects on the variations of compressive strengths of the delaminated composite panel. But, the compressive strengths of the panels having different delamination sizes at H/2 laminate thickness are more than that at H/3 and increase linearly with increase in delamination sizes.

**Keywords**— Composite structure, Delamination, Compressive strength, Finite element analysis, FEA

## I. INTRODUCTION

The use of composite materials in aircraft structural components has increased in the past few decades as a result of the many advantages they offer compared to metals. But

when composite airframe is put in service there are possibilities of accidental damages like tool drop, bird impact, foreign object damage (FOD) such as hail storm, stone hitting which may lead to delamination which is predominant mode of failure in composites. In many cases, the delamination will not grow and will result in only small stiffness degradation to the structure. This is especially true in tension load cases. In compression, delaminations can allow a sublaminar of the composite to buckle, which further drives the delamination growth. This failure mechanism, if not accounted for, can lead to uncontrolled delamination growth and premature failure of the structure. So the study of extent of delamination, growth, stability and its effect on compressive strength of composite structure becomes very important.

## II. PROBLEM STATEMENT

FEA analysis of composite panels with inbuilt delaminations has been carried out using ABAQUS FE code. Two configurations, one curved and other flat have been analysed. Firstly, the critical load of the laminate (without delamination) for buckling was predicted using a linear buckling analysis for the first Eigen value. Standard subspace method [1] was used for Eigen value extraction. Then delamination growth study was carried out using mixed mode fracture criteria.

The geometry and dimensions of the composite panel with a delamination have been shown in Fig. 1. The material used is Graphite Epoxy (AS4/3501-6) and Teflon the mechanical properties are shown in Table I taken from [2]. The nomenclature followed in the paper is as listed in the Table II.

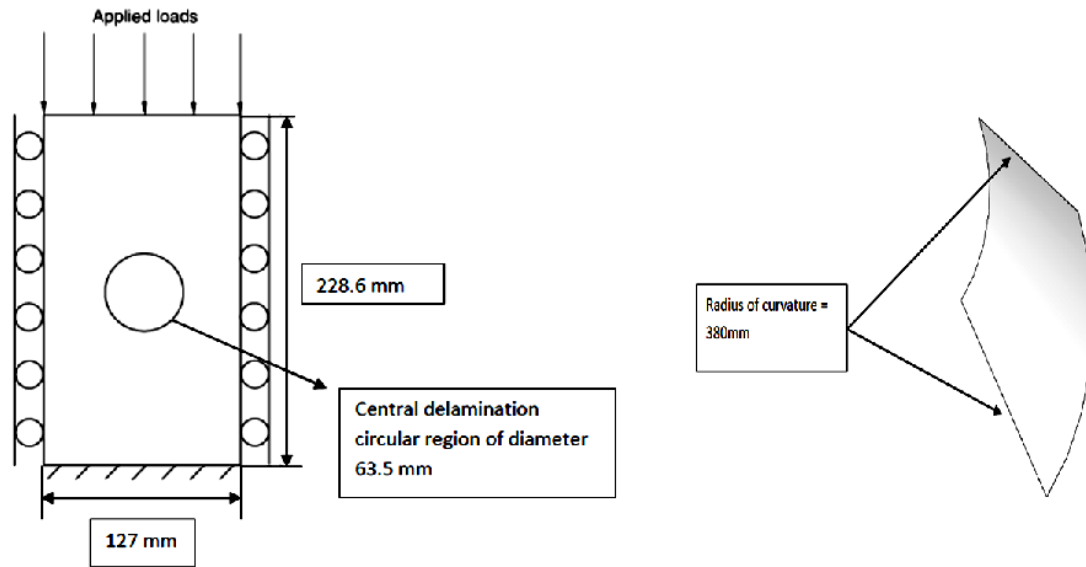


Fig. 1 Flat Composite Plate and Curved Composite Plate with Central Delamination

TABLE I  
MATERIAL PROPERTIES

S.no	Material property	Graphite Epoxy (AS4/3501-6)	Teflon
		Values	
1	$E_1$	127.554 e3 Mpa	1275.54 Mpa
2	$E_2$	11.307 e3 Mpa	113.07 Mpa
3	$G_{12}$	6.005 e3 Mpa	60.05 Mpa
4	$G_{13}$	6.005 e3 Mpa	60.05 Mpa
5	$G_{23}$	3.599 e3 Mpa	33.95 Mpa
6	$\nu_{12}$	0.30	0.30
7	$G_{Ic}$	82.07 J/mm <sup>2</sup>	
8	$G_{IIc}$	555.46 J/mm <sup>2</sup>	
9	$G_{IIIc}$	555.46 J/mm <sup>2</sup>	
10	Orientation type	$[(\pm 45/90/0)_2/\pm 60/\pm 15]_s$	
11	Ply thickness	0.13589 mm	
12	Total thickness	3.26136 mm	

S.no	Material property	Graphite Epoxy (AS4/3501-6)
		Values
13	Interface 1	-45/45/90/0// -45/45/90/0/-60/60/-15/15/15/-15/60/-60/0/90/45/-45  0/90/45/-45
14	Interface 2	-45/45/90/0// -45/45/90/0/-60/60/-15/15/15/-15/60/-60/0/90/45  -45/0/90/45/-45

### III. FINITE ELEMENT MODELLING

Finite element models of the specimen to be tested were created with 3D shell elements in the ABAQUS code. The delamination has been modelled in between 4<sup>th</sup> & 5<sup>th</sup> (Interface 1) for model validation of curved plate and in between 5<sup>th</sup> & 6<sup>th</sup> Ply (Interface 2) for the flat plate. The element type used is S4R and delamination region is modelled using two superimposed shell elements with contact constraints defined to prevent penetration of elements and the nonlinear FEA has been carried out. Table III shows the details of finite element model

TABLE III  
NOMENCLATURE

Symbol	Units	Description
$\sigma_1$	MPa	Stress along Principal fiber direction or direction 1 axis
$\sigma_2$	MPa	Stress perpendicular to fiber direction or direction 2 axis
$\tau_{12}$	MPa	Shear stress in 1-2 plane
$\sigma_x$	MPa	Stress along laminate coordinate x-direction
$\sigma_y$	MPa	Stress along laminate coordinate y-direction
$\tau_{xy}$	MPa	Shear stress in x-y plane
$X_t$	MPa	Allowable stress in tension in longitudinal direction (or 1-direction or fibre direction)
$X_c$	MPa	Allowable stress in compression in

		longitudinal direction
$Y_t$	MPa	Allowable stress in tension in transverse direction (or 2-direction or matrix direction)
$Y_c$	MPa	Allowable stress in compression in transverse direction
$S$	MPa	Allowable stress in shear (positive and negative shear has the same allowable)
$E_1$	MPa	Modulus of Elasticity along principal fiber direction
$E_2$	MPa	Modulus of Elasticity along in- plane perpendicular to fibers.
$E_3$	MPa	Modulus of Elasticity along Out of Plane perpendicular to fibers.
$E_x$	MPa	Modulus of elasticity along material x- direction
$E_y$	MPa	Modulus of elasticity along material y- direction
$E_z$	MPa	Modulus of elasticity along material z- direction
$G_{12}$	MPa	Rigidity modulus in 1-2 direction
$G_{23}$	MPa	Rigidity modulus in 2-3 direction
$G_{xy}$	MPa	Rigidity modulus in x-y direction
$G_{yz}$	MPa	Rigidity modulus in y-z direction
$G_I, G_{II}, G_{III}$	J/mm <sup>2</sup>	Strain energy release rate for Mode 1,2,3
$G_{TC}$	J/mm <sup>2</sup>	Total Critical Strain energy release rate
$G_{IC}, G_{IIC}, G_{IIIC}$	J/mm <sup>2</sup>	Critical strain energy release rate for Mode 1,2,3
$\nu_{12}$		Major poisson's ratio or poisson's ratio in 1-2 direction
$\nu_{21}$		Minor poisson's ratio or poisson's ratio in 2-1 direction
$\nu_{23}$		poisson's ratio in 2-3 direction

TABLE III  
MESH DETAILS

Number of nodes	3882
Number of elements	3840
Type of element	S4R (4-node general-purpose shell, reduced integration)
Element size in radial direction at the delamination front	1.9mm
Element size along circumferential direction	0.5mm
In the outer regions the Element size	7.143mm

#### IV. RESULTS AND DISCUSSION

The variation of  $G_t$  for the curved specimen with a delamination at the interface 1 is shown in the Fig. 2. The peak value for SERR occurs at a point along the delamination boundary measuring 7 deg (and 187 deg) for the values taken from reference [2] and peak values of 156

deg (and 336 deg) from the X axis are the values extracted from FEM analysis. The reference values and SERR values found along delamination front are following a very similar trend which validates the FEM analysis performed. The occurrence of peak values is due to the fact that SERR is a function of stress, and the stress concentration factor at those points are greater and hence the variation of SERR along delamination front is somewhat like sine curve as seen in Fig. 2. In the Fig. 3 cut view of delaminated composite panel can be observed which is difficult to observe in full view.

It is also seen from the figure 4 that failure loads decreases with increase in delamination sizes when the delamination is located at  $H/2$  distance i.e., at the mid thickness. The rate at which this decrease in failure load takes place is significant. However, for the delamination located at  $H/3$  thickness, the failure loads remain more or less same or decreases and this decrease is insignificant. This might be due to load path being concentrated mostly towards the mid thickness of the composite laminate and very less load being transferred near the edges.

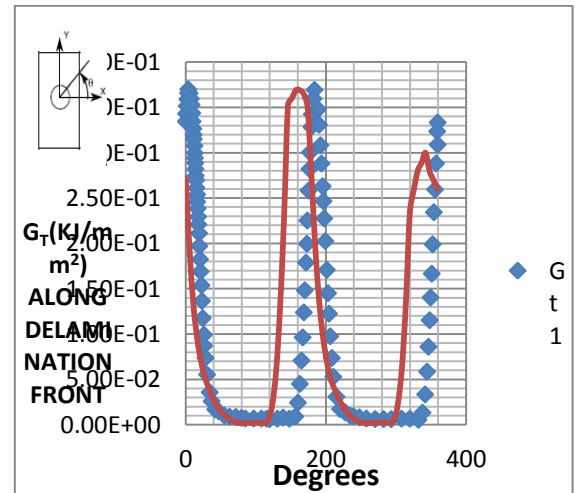


Fig. 1 Variation of  $G_t$  around the delamination front

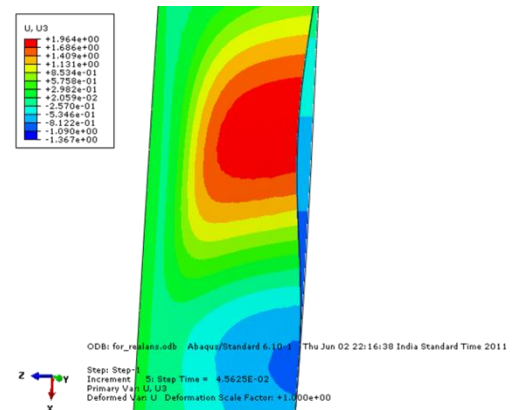


Fig. 3 Cut view along y-z plane showing internal delamination

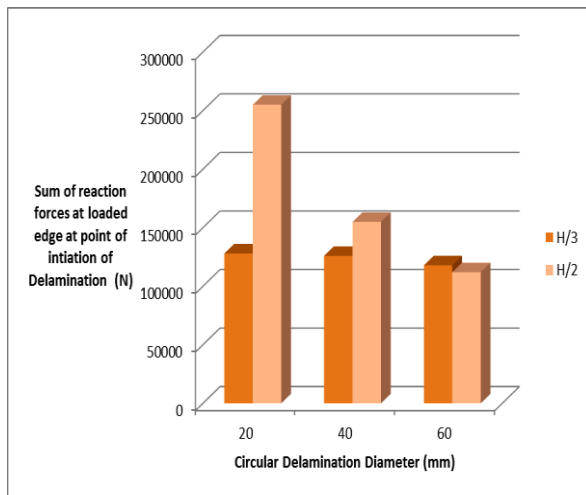


Fig. 4 Comparison of failure load found for delamination of different sizes and at different locations

## V. CONCLUSIONS

The linear buckling and nonlinear finite element analysis has been performed on both curved and flat composite panels with and without delamination respectively. The failure under compressive load is assumed to take place at the load when delamination initiates and was determined using SERR obtained from FEA in Conjunction with B-K's mixed mode fracture criterion. The predicted failure load corresponding to delamination initiation was found to be within 10% of the experimental value. Also, it was seen that predicted failure load at delamination initiation compares well with experimental value; whereas predicted buckling load did not correlate well with experimental buckling loads.

A nonlinear FE analysis has been performed and comparisons between predicted compressive strengths for laminates with different delamination geometries have been made. Failure loads has been obtained using SERR values from FE analysis in conjunction with B-K's fracture criterion. It was observed that failure loads decrease with the increase in delamination size at a particular location of laminate thickness. Also, it was observed that these values increase as the delamination is shifted towards mid-thickness of laminate. It was observed that the compressive strength of the embedded delamination decreases linearly with the increase in the size of delamination. The variation of delamination sizes at location H/3 laminate thickness does not have significant effect on the compressive strength.

## ACKNOWLEDGMENT

The support rendered by National Aerospace Laboratories and MVJ College of Engineering are kindly acknowledged.

## REFERENCES

- [1] Schoeppner, N.J. Pagano and G.A Delamination of Polymer Matrix Composites: Problems and Assessment s.l.: *Comprehensive Composite Materials*, Elsevier, 2000.
- [2] StinchComb, K. Schulte and W.W Delamiation of Polymer Matrix Composites problems and assessment. S. s.l.: Eleviser, 1989, Vol. 6.
- [3] Marom G ,Enviornmental Effects on Fracture Mechanical Properties of Polymer Composite Materials.. s.l.: *Composite material series* , 1985, Vol. 6.
- [4] Nairn, J.A ,Polymer composites .. 1985, Vol. chapter 6.
- [5] Clarke, M.J. Pavier and M.P ,Experimental Techniques for the investigation of the Effects of impact Damage on Carbon fiber Composites.. s.l.: *Composite Sciences and technolgy*, 1995, Vol. 55.
- [6] Liu., S.F. Hwang and G.H Buckling behaviour of Composite Laminates with multiple delaminatons under uniaxial compression s.l.: *Composite Structures*, 2001, Vol. 53.
- [7] Oswald, A. Tafreshi and T, Global buckling Bheviour and local Damaeg Propogation in Composite Plates With Embedded Delamination's.. s.l.: *Interanational journal of pressure vessels and Piping*, 2003, Vol. 80.
- [8] Cordisco, C. Bisagni and P Testing of Stiffened composite cylindrical shells in the post buckling Range until failure, 9, s.l.: *AIAA Journal*, 2004, Vol. 42.
- [9] Bolotin, V.V, Delaminations in composites structures: Its origin, buckling, growth and stabilty. 2, s.l.: *Composites:Part B Engineering*, 1996, Vol. 27.
- [10] Bolotin, V.V , Mechanics of Delaminations in laminate composite structures. s.l.: *Mechanics of composite materials*, 2001, Vol. 37.